The SRG RAT® supports human cell xenotransplantation through enhanced tumor microenvironment interactions

Caitlin M. O'Connor[1,2], Kaitlin P. Zawacki[1], Jessica R. Durrant[3], Kelsey Barrie[1], R. Grace Walton[4], Dana King[5], Gabrielle Hodges Onishi[1], Fallon K. Noto[4], Matthew Hinderman[1], Diane Begemann[4], Taylor Branyan[3], Kristin Panwell[3], Analisa DiFeo[6], Michael J. Schlosser[4], Goutham Narla[1,2*]

[1]Department of Internal Medicine: Division of Genetic Medicine, University of Michigan, Ann Arbor, Michigan.[2]Rogel Cancer Center, University of Michigan, Ann Arbor, Michigan. [3]DTR Labs, Farmers Branch, Texas.[4]Hera BioLabs Inc., Lexington, Kentucky.[5]BCRF Bioinformatics Core, University of Michigan, Ann Arbor, Michigan [6]Department of Pathology, University of Michigan, Ann Arbor, Michigan.

MICHIGAN MEDICINE
UNIVERSITY OF MICHIGAN

Abstract #6501

ABSTRACT

Background:
The use of immunodeficient mice for human tumor engraftment is an essential model of human cancer. However, low engraftment rates, slow growth, and smaller tumor volumes can be limitations. Previously, we reported a highly immunodeficient rat strain developed by Hera BioLabs, with the functional deletion of Rag2 and Il2rg genes on the Sprague-Dawley background (**SRG RAT®**). We have shown that the SRG rat supports the growth of multiple PDX and CDX models, however, the mechanisms underlying the supportive growth are not fully understood. Additionally, direct comparison of engraftment rates and tumor growth between the SRG rat and NSG mice is limited.

Methods:
Here, we subcutaneously engrafted two CDX and five PDX models into SRG or NSG animals and tracked tumor growth. In all cases, the engraftment and tumor growth rates were better supported in the SRG rat compared to the NSG mouse. Interestingly, the SRG rat is not more immunocompromised than the NSG mouse, suggesting alternative mechanisms supporting growth in the SRG. To understand this, we explored the tumor microenvironment (TME) between models grown in the two host animals. We analyzed tumors from the H660 CDX model of castrate-resistant prostate cancer grown in either SRG rats or NSG mice using markers of the TME via immunohistochemistry.

Results:
In summary, the data show that the SRG rat supports the growth of various human cancer types and exhibits improved tumor microenvironment interactions compared to NSG mice. Furthermore, the more developed stromal and vascular compartments of tumors grown in SRG rats were closer to the architecture of the original patient tumors, emphasizing the potential of the SRG rat as a valuable model for human cancer.

Study Name	Type	Engraftment Rate SRG	Engraftment Rate NSG	Time to Engraftment SRG	Time to Engraftment NSG
TM00233 Lung Adenocarcinoma	PDX	3/3 (100%)	5/5 (100%)	70d	63d
J000096652 Lung Adenocarcinoma	PDX	2/2 (100%)	3/5 (60%)	16d	26d
J000112358 Uterine Endometrioid Carcinoma	PDX	3/3 (100%)	5/5 (100%)	76d	69d
TM00001 Uterine Sarcoma	PDX	3/3 (100%)	3/5 (60%)	55d	181d
TM00274 Uterine Leiomyosarcoma	PDX	3/3 (100%)	5/5 (100%)	34d	83d
PDX133 Ovarian Carcinosarcoma	PDX	2/2 (100%)	5/5 (100%)	32d	63d
PDX111 High-grade serous carcinoma (Ovarian)	PDX	2/2 (100%)	3/5 (60%)	90d	160d
EFO-27 Ovarian Adenocarcinoma	CDX	3/3 (100%)	5/5 (100%)	35d	35d
NCI-H660 Neuroendocrine Prostate Carcinoma	CDX	5/5 (100%)	5/5 (100%)	41d	48d

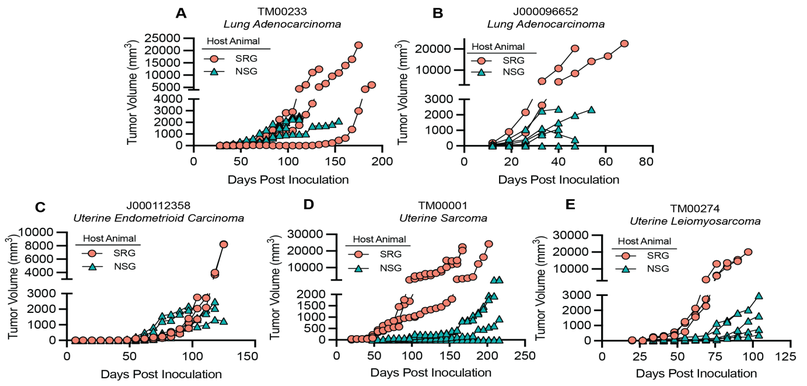

Figure 1: SRG rats support the growth and engraftment of multiple PDX and CDX models over conventional immunodeficient mice. **A,** 8 mm^3 fragments of lung adenocarcinoma PDX TM00233 were implanted subcutaneously into NSG mice (n=4) or SRG rats (n=3). **B,** 8 mm^3 fragments of lung adenocarcinoma PDX J000096652 were implanted subcutaneously into NSG mice (n=5) or SRG rats (n=2). **C,** 8 mm^3 fragments of uterine carcinoma PDX J000112358 were implanted subcutaneously into NSG mice (n=5) or SRG rats (n=3). **D,** 8 mm^3 fragments of uterine sarcoma PDX TM0001 were implanted subcutaneously into NSG mice (n=5) or SRG rats (n=3). **E,** 8 mm^3 fragments of uterine leiomyosarcoma PDX TM00274 were implanted subcutaneously into NSG mice (n=5) or SRG rats (n=3

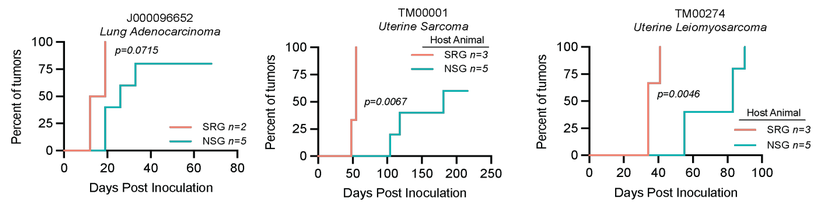

Figure 2: Time to tumor engraftment for PDX and CDX studies. **A-C,** Tumor volumes were measured by caliper measurement. Positive engraftment was considered when tumors were palpable and reached 200 mm^3. If tumors were under 200mm^3 at the end of the study, animals were censored at that time. 8 mm^3 fragments of tumor tissue was implanted unilaterally into NSG mice (n=5) or SRG rats (n=2 or 3) for each of the following: **A,** lung adenocarcinoma PDX J000096652 **B,** 8 mm3 fragments of uterine sarcoma PDX TM0001 **C**, 8 mm3 fragments of uterine leiomyosarcoma PDX TM00274. p-values were determined by Log-rank (Mantel-Cox) test.

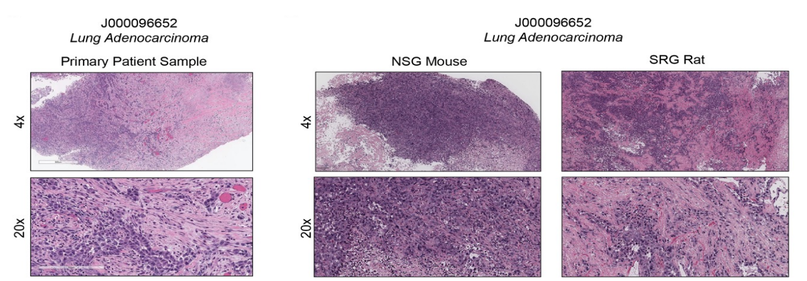

Figure 3: Lung adenocarcinoma PDX models grown in the SRG rat display a microenvironment that more closely represents the originating patient tumor. **A**, H&E images from the primary patient sample where the J000096652 PDX was derived, 4X magnification (top), 20X magnification (bottom). Scale bars indicate 200 μm (20x) and 600 μm (4x). Images from The Jackson Laboratory's Mouse Tumor Biology Database. **B**, Representative images from J000096652 tumors grown in the NSG mouse (left) or SRG rat (right). 4X magnification (top), 20X magnification (bottom). Scale bars indicate 50 μm (20x) and 250 μm (4x).

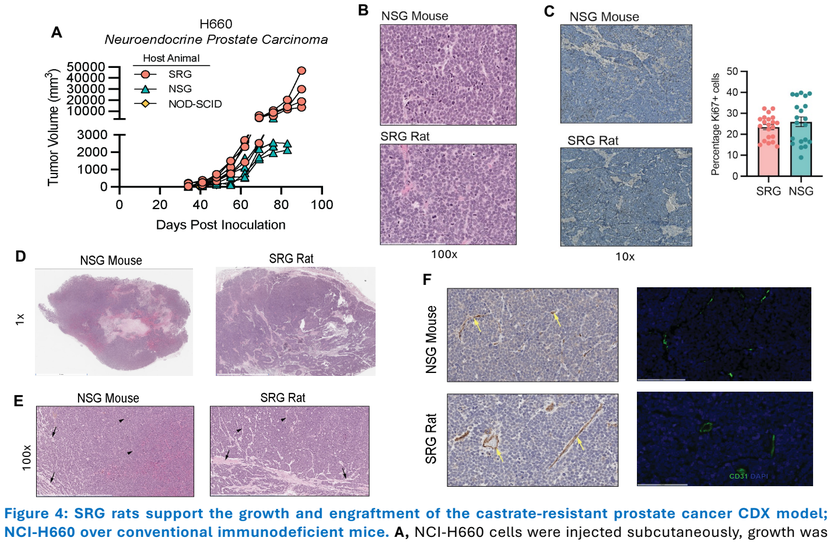

Figure 4: SRG rats support the growth and engraftment of the castrate-resistant prostate cancer CDX model; NCI-H660 over conventional immunodeficient mice. **A,** NCI-H660 cells were injected subcutaneously, growth was tracked by caliper measurement. **B,** Representative H&E tumor cross sections (400x); scale bar indicates 200 μm, shows morphology and mitotic count of the NCI-H660 cells to be equivalent between the species **C**, Representative images (10x); scale bar indicates 100 mm and quantification of the Ki67 staining by IHC of tumors (n=4 tumors from each host species were used for the analysis). **D**, Representative H&E image (1x) of a tumor grown in the NSG mouse (left) or SRG rat (right). Scale bar indicates 5 mm. **E**, Representative H&E images (100x) of tumor stroma show fibrovascular stroma (black arrowheads) and dense collagen/ECM tracts (black arrows). Scale bar indicates 1 mm. **F**, Chromogenic CD31 staining (left), and fluorescent CD31 (right) immunoreactive blood vessels tend to be smaller and more numerous in mouse tumor tissue, with larger more sparce blood vessels supported by more abundant stroma in rat tumor tissue. Scale bar indicates 20 μm

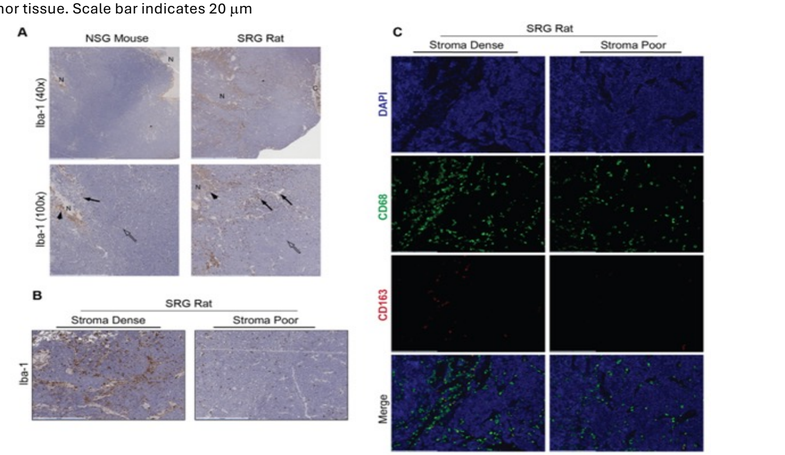

Figure 5: NCI-H660 tumors grown in the SRG rat show activated macrophages in stroma-dense regions. All slides were obtained serially from the section used for Xenium analysis **A**, Iba-1 immunolabeling of macrophages by DAB chromogen in mouse (left) and rat (right) tumors. Macrophages adjacent areas of necrosis (black arrowhead), in areas of abundant stroma (black arrows) and less stroma (open arrows) are shown. Areas of necrosis (N), capsule (C), denser stroma (*) are indicated. Scale bar indicates 2 mm (4x; top row) and 1 mm, 10x; bottom row). Quantification can be found in Supplemental Figure 12. **B**, Iba-1 immunolabeling of macrophages by DAB chromogen in stroma-dense (left) or stroma-poor (right) regions of tumors taken from the SRG rat. Scale bar indicates 500 mm (10x). **C,** CD68/CD163 dual IF for macrophages in stroma-dense and stroma-poor regions of SRG rat. DAPI: top row, CD68 (green channel), CD163 (red channel), Merged image: bottom row; CD68+CD163+ cells are yellow. Scale bar indicates 200 mm (30x).

Hera BioLabs

DTR LABS
DALLAS • BOSTON

bioRxiv
THE PREPRINT SERVER FOR BIOLOGY